

24 **Summary**

- 25 • Extreme weather events are increasing in frequency and intensity due to global climate
26 change. We hypothesized that these have a strong impact on the stem radial growth and the
27 dynamic of non-structural carbohydrates (NSCs).
- 28 • In order to assess the effects on mature trees of a late frost occurred in spring 2016 and a
29 drought event characterizing the summer 2017, we monitored the phenology, the radial
30 growth and the dynamic of starch and soluble sugars in a Mediterranean beech forest.
- 31 • Growth was much more reduced by spring late frost than by summer drought, while NSCs
32 dynamic was deeply involved in counteracting the negative effects of both events,
33 supporting plant survival and buffering source-sink imbalances under such stressful
34 conditions, resulting in a strong trade-off between growth and NSCs dynamic in trees.
- 35 • Overall, our results highlight the key role of NSCs on trees resilience to extreme weather
36 events, confirming the relevant adaptability to stressful conditions. Such an insight is useful
37 to assess how forests may respond to the potential impacts of climate change on ecosystem
38 processes and to define how future management strategies can help adaptation of beech
39 forests in the Mediterranean area.

40
41 *Keywords: Carbon allocation, Carbon reserves, Drought, Fagus sylvatica L., Late frost,*
42 *Mediterranean, Phenology, Resilience*

43 **Introduction**

44 Global climate change is causing an increment in the frequency of extreme weather events
45 (Stocker *et al.*, 2014) that are recognized among the major drivers of current and future ecosystem
46 dynamics (Frank *et al.*, 2015). The Mediterranean basin is one of the two main hot-spots of climate
47 change (Giorgi, 2006; Noce *et al.*, 2017), showing increases in the inter annual variability and of
48 extreme environmental conditions (Flaounas *et al.*, 2013). In this region, the increasing risk of late
49 frost events represents one of the major threats associated with the future global change (Zohner *et*
50 *al.*, 2020). Indeed, increasing spring temperatures has been observed stimulating earlier leaf
51 unfolding (Gordo & Sanz, 2010; Allevato *et al.*, 2019), thus potentially exposing young leaves and
52 shoots to spring frost damage (Augspurger, 2013), especially at high elevation (Vitasse *et al.*,
53 2018). Depending on species, temperatures below -4°C can destroy the “fresh” leaves and shoots
54 reducing – up to even blocking – the photosynthetic capacity of trees for several weeks. In this
55 case, the resource requirements for new leaves formation, and tree life maintenance, must
56 necessarily rely on the remobilization of carbon (C) reserves (Dittmar *et al.*, 2006; D’Andrea *et al.*,

57 2019). Moreover, severity, duration, and frequency of drought events have all been increasing in the
58 last decades (Spinoni *et al.*, 2015). European beech (*Fagus sylvatica* L.), one of the most diffused
59 native tree species in Europe, is known to be drought sensitive (Bolte *et al.*, 2016). Hence, drought
60 events can negatively affect physiological performance (Rezaie *et al.*, 2018), carbon allocation
61 (D'Andrea *et al.*, 2020a), reproductive capacity (Nussbaumer *et al.*, 2020), as well as the growth
62 and competitive strength of the species (Peuke *et al.*, 2002) which may all impact its future
63 distribution (Noce *et al.*, 2017).

64 Growth and non-structural carbohydrates (NSCs; i.e. sucrose, fructose, glucose and starch)
65 dynamic are among the most strongly affected ecosystem processes by spring frost and summer
66 drought (Li *et al.*, 2018). An increasing body of evidence has shown that NSCs dynamic is not a
67 pure passive deposit and removal of C compounds, but it represents a key process actively
68 controlled by plants to finely regulate C source-sink balance and to buffer the difference between C
69 supply and demand at different timescales (Scartazza *et al.*, 2001; Sala *et al.*, 2012; Carbone *et al.*,
70 2013; Fatichi *et al.*, 2014; Moscatello *et al.*, 2017; Collalti *et al.*, 2020). Therefore, NSCs could play
71 a crucial role in counteracting the negative effects of extreme weather events on beech forests,
72 contributing to their resilience and survival (Scartazza *et al.*, 2013; D'Andrea *et al.*, 2019).
73 Unfortunately, despite the recognized importance of NSCs for plant productivity and resilience,
74 little is known regarding their seasonal regulation and trade-off with growth and reproduction in
75 forest trees (Merganičová *et al.*, 2019; Tixier *et al.*, 2020).

76 In this work, we studied the effects of spring late frost and summer drought in a long-term research
77 plots established on a Mediterranean beech forest of Central-South Italy (Collelongo, Abruzzi
78 Region, Italy). The site is located in the large area in the Central-South Italy where in spring 2016,
79 due to unusually warm preceding weeks, leaf unfolding occurred up to 15-20 days earlier than the
80 normal average, followed by frost, that caused the complete loss of the newly grown canopy.
81 Moreover, in 2017, a strong summer drought, due to a combination of drastic reduction of
82 precipitation associated with high air temperature in late July and August, interested a huge area of
83 the Mediterranean basin (Bascietto *et al.*, 2018; Nolè *et al.*, 2018; Allevato *et al.*, 2019; Rita *et al.*,
84 2019), including the Collelongo site. Notwithstanding these events were monitored through remote
85 sensing techniques, *in situ* evaluations of their effects on ecosystem functionality are limited.
86 Phenology, growth and NSCs dynamic in the Collelongo beech stand were investigated during 2016
87 (i.e. the year of the late frost event) and 2017 (i.e. the year of the summer drought event) and
88 compared to the historical inter-annual data collected earlier at the site.

89 The objectives of the study were to: *i*) quantify the magnitude of the effects of such extreme
90 events on ecosystem functioning; *ii*) verify the role of NSCs in mediating source-sink balance

91 following the strong alteration of C activity; *iii*) evaluate the interplay and trade-off between carbon
92 allocation to canopy, stem and C reserves. The aim was to predict how these responses and
93 regulation processes could contribute to the resilience of beech to extreme weather events
94 associated with future global change.

95 **Material and methods**

96 **Study site**

97 The study was carried out during the years 2016 and 2017 in an even-aged, pure beech forest
98 (*Fagus sylvatica* L.) located at Selva Piana stand (41°50'58" N, 13°35'17" E, 1560 m elevation) in
99 the Central Apennine (Collelongo, Abruzzi Region, Italy). The experimental area is included in the
100 LTER network (Long Term Ecological Research) and more specific information about the site were
101 already reported in previous works (Guidolotti *et al.*, 2013; Collalti *et al.*, 2016; Rezaie *et al.*, 2018;
102 Reyer *et al.*, 2020) in which the soil, forest structure, and climate characteristics are described.

103 **Climate and Phenology**

104 The temperature and precipitation for the period 1989-2015, available on the Fluxnet2015
105 release, were used to characterize the, on average, climate conditions of the site. For the data gaps
106 occurred during the experimental trial (2016-2017), we used the ERA5 database produced by the
107 European Centre for Medium-Range Weather Forecasts (ECMWF)
108 (<https://www.ecmwf.int/en/forecasts/datasets/archive-datasets/reanalysis-datasets/era5>, data
109 accessed: [12/04/2018]), according to the Fluxnet2015 release formulations (Pastorello *et al.*, 2020).
110 To evaluate peculiarities of the climatic conditions in 2016 and 2017 we calculated monthly
111 differences with respect to the average values of precipitation and temperature observed in the site
112 in the historical time series 1989-2015.

113 Leaf phenology was monitored using the MODIS Leaf Area Index product (LAI, MOD15A2H
114 product, <https://modis.gsfc.nasa.gov/>) with 8-day temporal resolution and 500-meter spatial
115 resolution (Myneni *et al.*, 2015). Critical dates, representing approximately linear transitions from
116 one phenological phase to another, were identified and defined according to Zhang *et al.* (2003) as:
117 (1) *green-up*, photosynthetic activity onset; (2) *maximum LAI*, supposed to be the leaf maturity
118 phase; (3) *senescence*, sharp decrease of photosynthetic activity and green leaf area; (4) *winter*
119 *dormancy*. In 2016, the leafless period after the late frost was identified from the day of the extreme
120 event and the second green up.

121 **Selection, measurements and sampling of trees**

122 Five trees were selected according to their similarity with site tree ring chronology, the trees
123 had diameters at breast height (DBH) ranging from 49 to 53 cm (for more details see D'Andrea *et*

124 *al.* 2020b). Trees were monitored from April 2016 to November 2017. Intra-annual radial growth of
125 each selected tree was measured using permanent girth bands with 0.1 mm accuracy (D1 Permanent
126 Tree Girth, UMS, Germany). Furthermore, stem diameter was recorded at the moment of each
127 sampling of xylem for biochemical analyses (20 sampling dates from April 2016 to November
128 2017).

129 From each tree, micro-cores (2 mm diameter, 15 mm long) of wood were collected after bark
130 removal, using the Trephor tool (Rossi *et al.*, 2005). All samples for biochemical analyses were
131 immediately placed in dry ice for transport to the laboratory, then stored at $-20\text{ }^{\circ}\text{C}$ and, finally,
132 stabilized through lyophilisation processes until NSCs analysis.

133 Daily radial increment (R_i , $\mu\text{m day}^{-1}$), was calculated as follow:

134

$$135 \quad R_i = \frac{R_t - R_{t-1}}{\Delta t} \quad \text{eq.1}$$

136

137 where R is the radius of each i tree (μm), t is the date of sampling, and Δt is the time interval
138 between the two sampling dates expressed in days.

139 In November 2017, at the end of the experimental trial, increment cores were collected at breast
140 height from each tree, using an increment borer. Tree ring width series were converted into tree
141 basal area increment (BAI, $\text{cm}^2 \text{ year}^{-1}$), according to the following standard formula:

142

$$143 \quad BAI = \pi (R_n^2 - R_{n-1}^2) \quad \text{eq.2}$$

144

145 with n being the year of tree-ring formation.

146

147 **Starch and soluble sugar concentrations analysis**

148 The freeze-dried xylem samples were milled to a fine powder and used for all analytical
149 tests. For analysis of glucose, fructose, sucrose and starch, 10 mg of dry xylem powder were
150 extracted in 1 ml of 80% ethanol/water at $80\text{ }^{\circ}\text{C}$ for 45 minutes. After centrifugation at $16,000 \times g$
151 for 5 minutes, soluble sugars were recovered in the supernatant while the pellet was resuspended in
152 1 ml of 40 mM acetate buffer (pH 4.5), then re-centrifuged $16,000 \times g$ for 5 minutes. This procedure
153 was repeated 4-times. The final pellet was autoclaved for 45 minutes at $120\text{ }^{\circ}\text{C}$ in the same wash
154 buffer. Enzymatic starch hydrolysis and the following glucose spectrophotometric assay were done
155 as described by Moscatello *et al.* (2017). The supernatant solution containing soluble sugars was
156 filtered on $0.2\text{ }\mu\text{m}$ nylon filters (GE-Whatman, Maidstone, UK), then analyzed by high-performance
157 anion exchange chromatography with pulsed amperometric detection (HPAEC-PAD) (Thermo

158 Scientific™ Dionex™ ICS-5000, Sunnyvale, CA U.S.A.)(Proietti *et al.*, 2017).

159

160 **Modelling of Intra-annual dynamics of non-structural carbohydrates**

161 To evaluate the effects of the spring late frost (2016) and the heat wave and drought stress
162 (2017) on the intra-annual NSCs dynamic, a representative benchmark of the typical intra-annual
163 carbohydrates dynamic of the study site was needed. With this aim, a dataset on NSCs dynamic
164 derived from other experimental trials at the site was used (Supporting Information Table S1).
165 Dataset was composed of data of different years (i.e.: 2001, 2002, 2013, 2014, 2015, and 2018).
166 This dataset included 39 observations of starch dynamic and 28 observations for both soluble sugars
167 (glucose, fructose and sucrose) and total NSCs dynamic. Observations for soluble sugars were
168 lower, because of the methodological sampling procedure used in 2015. During that year, woody
169 samples were collected for xylogenesi analysis and maintained in ethanol-formalin acetic acid
170 solution (FAA). Unfortunately, this methodology caused the loss of soluble sugars, while the starch
171 integrity was preserved, as verified by means of specific analytical tests on woody tissues.

172 Different models based on data of starch, soluble sugars and total NSCs were used looking
173 for possible patterns within the years and tested through the Akaike Information Criterion (AIC)
174 (Akaike, 1974; Aho *et al.*, 2014) to select the simplest model able in reproducing the *in situ*
175 observed pattern. The AIC quantifies the trade-off between parsimony and goodness-of-fit in a
176 simple and transparent manner, estimating the relative amount of information lost by a given model.
177 Hence, the model showing the lowest AIC is considered the model with the smallest information
178 loss and, potentially, the most representative one (Akaike, 1974). The four assumptions of linear
179 model (homoscedasticity, normality of the error distribution, statistical independence of the errors
180 and absence of influential points) were tested graphically (Fig. S1). Statistical analysis and figures
181 were made using R 3.5.0 (R Development Core Team, 2018).

182 **Results**

183 **Climate in the study period**

184 Monthly variations of temperature and precipitation in the Selva Piana beech forest are
185 reported in Figure 1a-b. In 2016 a severe late frost event occurred during the night between April 25
186 and 26, when the temperature at canopy level (~ 24 m) reached – 6 °C (Fig. 1a inset panel). The
187 extreme frost event followed an early spring season characterized by a temperature that during the
188 months of February and April was significantly higher (about 2°C) than the average value of the
189 site for the period 1989-2015 (Fig. 1a). In 2017, from May to August, the temperature was
190 significantly higher than the average value of the site, with an increase of ~3 °C (Fig 1a).

191 Furthermore, from May to October 2017 a significant reduction of precipitation against long term
192 average was observed (Fig. 1b), leading to an annual precipitation that was ~ 50% of the 1989-2015
193 average (Fig. 1b inset panel).

194

195 **Phenological parameters and radial growth**

196 The seasonal LAI trend, used to define the phenological phases of the stand, is reported in
197 Fig. 2a. The “first” green up in spring 2016 occurred between 20 and 30 days earlier than the
198 average of the site (Fig. 2a), while the “second” (re)green up, after the complete canopy destruction
199 due to the spring frost event, started around June 28, with a leafless period of more than 60 days. In
200 2016 the beginning of the senescence phase was anticipated of about one week compared to the
201 average of the long-term series (Fig. 2b). Maximum LAI was lower in 2016 ($LAI = 4.79 \text{ m}^2 \text{ m}^{-2}$)
202 than in 2017 ($LAI = 5.37 \text{ m}^2 \text{ m}^{-2}$), while the long-term average LAI of the site assessed with remote
203 sensing was $\sim 5 \text{ m}^2 \text{ m}^{-2}$ (Fig. 2a). The average length of vegetative period assessed through remote
204 sensing during the 2000-2015 period was approximately 140 days, a value confirmed in 2017, while
205 it was 83 days in 2016.

206 The mean BAI in the 2000-2015 period was $22.64 \pm 0.78 \text{ cm}^2 \text{ year}^{-1}$, while it was $3.69 \pm$
207 $1.14 \text{ cm}^2 \text{ year}^{-1}$ and $18.75 \pm 3.80 \text{ cm}^2 \text{ year}^{-1}$ in 2016 and 2017, respectively (Fig. 2b inset panel).
208 The late frost in spring 2016 reduced the stem radial growth of about 85% compared to the average
209 of the period 1989-2015. The late frost strongly affected the seasonal dynamic of stem diameter
210 growth during the year 2016, as shown by the lower and almost constant rate of stem growth
211 compared to 2017, when after the green up the radial growth followed the usual pattern, reaching
212 the highest increment ($32.30 \pm 4.14 \text{ } \mu\text{m day}^{-1}$) in July (Fig. 2b).

213

214 **Intra-annual dynamic of NSCs**

215 The values and the modelled intra-annual dynamics of NSCs (total sugars, starch and
216 soluble sugars content) measured in the beech stem wood are reported in Fig. 3 (panels a, b and c).
217 Dynamic of NSCs showed polynomial equation patterns at different grades, with R^2 ranging from
218 0.64 to 0.93 (Table 1). Comparing the modelled NSCs intra-annual dynamics and stand phenology,
219 an increase in total NSCs is observed from the bud break to the beginning of green-up phase, due to
220 the increasing starch content notwithstanding the decrease of soluble sugars. During the period
221 between the onset and the middle of the maximum vegetative season, total NSCs content decreased
222 due to starch reduction, while the amount of soluble sugar remained unchanged. In the late summer,
223 both starch and soluble sugars increased until the end of the vegetative season, determining an
224 increase of total sugars content (Fig. 3a). At the beginning of dormancy phase, a decrease of total

225 NSCs was recorded, driven by a severe decrease of starch although associated with a simultaneous
226 increase in soluble sugars.

227 In 2016, the lowest soluble sugars content ($5.02 \pm 0.46 \text{ mg g}_{\text{DW}}^{-1}$) was measured close to the
228 build-up of the new photosynthetic apparatus. In the same year, the maximum soluble sugars
229 content ($15.29 \pm 0.48 \text{ mg g}_{\text{DW}}^{-1}$) was measured at the end of the vegetative season, during the
230 dormancy phase, while two peaks of starch content were measured after the canopy destruction
231 ($24.80 \pm 0.20 \text{ mg g}_{\text{DW}}^{-1}$) and close to the beginning of the senescence phase ($19.93 \pm 2.82 \text{ mg g}_{\text{DW}}^{-1}$).
232

233 In 2017, the lowest content of soluble sugars ($6.16 \pm 1.36 \text{ mg g}_{\text{DW}}^{-1}$) was measured at Day of
234 the Year (DOY) 186, while the lowest starch contents were measured before the green up ($13.82 \pm$
235 $1.51 \text{ mg g}_{\text{DW}}^{-1}$) and during the dormancy ($9.37 \pm 1.36 \text{ mg g}_{\text{DW}}^{-1}$).

236 Although the seasonal trends of carbohydrates accumulation in wood samples in 2016 and
237 2017, were similar to the modelled NSCs dynamic recorded in the reference period, some
238 substantial differences can be observed. In 2016, the higher starch content, balanced by a low
239 soluble sugars amount, was recorded soon before the green up. After the second leaf re-sprouting,
240 starch content decreased considerably, reaching a value lower than the modelled reference value at
241 the site. In August 2016, both starch and soluble sugars increased until leaves senescence, which
242 occurred earlier than the average of the site. After that, a reduction of the total carbohydrate
243 reserves was observed.

244 The lower amount of storage carbohydrates reached in 2016, directly affected the starch and
245 total NSCs amount recorded during the first part of the vegetative season in 2017, when a very low
246 content of starch and total carbohydrates was measured. At the end of July 2017, although the starch
247 content was lower than the modelled value of the site, a refilling of total carbohydrate reserves was
248 observed. The drought stress event of August 2017 strongly affected the composition of
249 carbohydrate reserves due to a severe starch hydrolysis, leading to a decrease of starch content of
250 about 35% and a parallel increase of soluble sugars. During the late phase of vegetative season of
251 2017, the carbohydrates pattern returned close to the modelled intra annual dynamic, although with
252 a limited reduction compared to the site average.

253 **Discussion**

254 **The buffering capacity of NSCs in response to the late frost**

255 As already observed at the site and as reported in the literature, the seasonal dynamics of
256 NSCs play a crucial role in regulating C source-sink balance through buffering the difference
257 between C supply and demand (Scartazza *et al.*, 2013; Fatichi *et al.*, 2014; Collalti *et al.*, 2018,

258 2020). The complete destruction of photosynthetic canopy and the strong reduction of stem radial
259 growth during springtime 2016 (May-June) following the frost event, were associated with an
260 increase of stemwood NSCs due to starch accumulation. An increase in total stemwood NSCs has
261 been previously observed from November to March in other temperate forests and it was attributed
262 to remobilization of sugars from storage compartments in coarse roots in advance of the C demands
263 associated with springtime growth (Hoch *et al.*, 2003; Hartmann & Trumbore, 2016). The NSCs
264 seasonal dynamic shows that starch accumulation in beech occurs during the formation of the new
265 crown, in the presence of the potentially dominating sink represented by new growing leaves and
266 shoots, while soluble sugars are decreasing. Furthermore, our results confirm that the accumulation
267 of starch in sapwood of beech trees during springtime is not necessarily supported by freshly
268 produced photosynthates. In 2016, it occurs, uniquely, as the result of the remobilization of already
269 existing soluble NSCs, including those remobilised from below-ground organs. The normal starch
270 rise in spring could be favoured by the destruction of the developing canopy leaves. This condition
271 leads to a high concentration of soluble sugars within the stemwood that, concurrently to the
272 springtime increased air temperatures, favour synthesis of starch over its degradation (Witt &
273 Sauter, 1994). Indeed, it was recently demonstrated in one-year old shoots of *Juglans regia* L. that
274 wood accumulation of starch can be increased when photosynthate export from the shoot is blocked
275 by girdling. In such case, the increase of starch accumulation is accompanied by an increase of the
276 total activity of ADPglucose pyrophosphorylase (Moscatello *et al.*, 2017), an enzyme well known
277 for its high control over starch synthesis. Thus, the spring programmed activation of starch
278 synthesis in wood can occur even when C resources are very limited by the absence of a
279 photosynthesizing crown. This strongly supports the hypothesis of an active control of the
280 accumulation and buffering role of NSCs in wood (Sala *et al.*, 2012; Collalti *et al.*, 2020).

281 The buffering role of NSCs to compensate the difference between C sink and C supply was
282 also particularly evident during the late spring and early summer 2016, when stemwood starch
283 reserves were partially hydrolysed for sustaining the second leaf re-sprouting, causing a slight
284 decrease of NSCs during July compared to the modelled values of the site. D'Andrea *et al.* (2019),
285 using the ¹⁴C bomb technique, found that up to 5 years old reserves can be mobilized to sustain the
286 tree metabolic activities and leaf re-sprouting after the frost damage, further supporting the role of
287 NSCs in the resilience of beech to extreme weather events such as late spring frost. This
288 information is crucial in understanding the resilience capacity of Southern beech forest to late frost,
289 especially considering that extreme warm events may have particularly strong influences at the end
290 of winter when some species interrupt dormancy and the risk of freezing remains relatively high
291 (Ladwig *et al.*, 2019). After the complete canopy defoliation subsequent to the frost event, cambium

292 activity was maintained at low rates, representing an additional C sink during the leafless period
293 fuelled by the stemwood reserves (D'Andrea *et al.*, 2020b). During the second part of the season
294 (August-September), the new assimilates from the canopy are mainly used to sustain C sink
295 activities related to wall thickening and lignification phase (Prislan *et al.*, 2018) and to refill the
296 starch reserves within the stemwood. However, C allocation to cell wall thickening, was extremely
297 limited in 2016 due to strong reduction of xylem cells production (D'Andrea *et al.*, 2020b). This
298 possibly led to the increase of both starch and soluble sugars observed in stemwood of beech plants
299 in August 2016, notwithstanding the reduction of the net ecosystem exchange (NEE) compared to
300 the 2000-2015 values (Bascietto *et al.*, 2018). The NEE decrease in 2016 is related to canopy
301 destruction after the late frost and, overall, to the lower LAI, likely associated also with a reduction
302 of photosynthetic efficiency of defoliated beech trees (Gottardini *et al.*, 2020). In that year, the
303 strong reduction of sink activity, concomitantly with the seasonal decrease of air temperatures,
304 could contribute to the slightly anticipated closure of the season. After leaf shedding, starch was
305 partly hydrolysed and converted to soluble sugars to reduce cell osmotic potential and induce cold
306 tolerance (Bonhomme *et al.*, 2005; Tixier & Sperling, 2015).

307 **The role of NSCs to face the summer drought**

308 The slight reduction of C reserves at the end of the 2016 growing season impacted the
309 dynamic of the following year. Notwithstanding that the content of starch showed the typical
310 seasonal trend of the site, the starch content in woody tissue from bud break till the end of June
311 2017 was clearly lower than the modelled reference NSCs dynamic of the site, while there were not
312 relevant differences among modelled and measured content of soluble NSCs. This phase was
313 followed by a sharp rise in the stem radial growth as typical for the site (Scartazza *et al.*, 2013). In
314 summer 2017, the warm drought event had a strong effect on NSCs dynamic, leading to starch
315 hydrolysis and accumulation of soluble sugars in woody tissue. As drought induces a partial
316 stomatal closure that reduces C uptake, trees are forced to depend more on NSCs storage to sustain
317 metabolic activities, defence mechanisms against pathogens and osmoregulation processes
318 (McDowell, 2011; Hartmann & Trumbore, 2016). The negative effects of drought can be
319 exacerbated by the concomitant temperatures higher than average (i.e. the so-called “hot” drought),
320 strongly affecting water transport between roots and canopy (Hartmann & Trumbore, 2016).
321 Moreover, respiration increases with temperature leading to NSCs depletion (Guidolotti *et al.*,
322 2013; Collalti *et al.*, 2018), while, at the opposite, drought alone reduces whole-plant and root
323 respiration (Hartmann *et al.*, 2013). The observed increase of wood soluble sugars concentration
324 during July-August 2017 is in agreement with the key role of these C compounds as compatible
325 solutes for osmoregulation (Chaves *et al.*, 2003). Indeed, plants under drought conditions can

326 actively control the osmotic cell pressure to avoid tissue dehydration and maintain the physiological
327 functions by increasing the concentration of different kinds of compatible solutes such as betaines,
328 amino acids and sugars (Morgan, 1984). In our study, the increased concentration of stemwood
329 soluble sugars during drought was due to both hexoses (glucose and fructose) and sucrose (data not
330 shown), according to previous findings (Fu & Fry, 2010; Yang, 2013). In addition, NSCs have also
331 a relevant role to maintain xylem transport and embolism repair under drought conditions
332 (Scartazza *et al.*, 2015; Hartmann & Trumbore, 2016). The so called ‘*C starvation hypothesis*’
333 (Mcdowell *et al.*, 2008) speculates that the drought-induced stomatal closure minimizes hydraulic
334 failure but, at the same time, causes a decline of photosynthetic uptake, possibly leading to C
335 starvation as carbohydrates demand continues for the maintenance of metabolism and defence.
336 Moreover, the concomitance of elevated temperatures could accelerate the starch depletion leading
337 to tree mortality (Adams *et al.*, 2009), suggesting that trees, to avoid this risk, should be able to
338 maintain a minimum (safety) level of reserve under drought and warm conditions (McDowell &
339 Sevanto, 2010). Our results support this hypothesis, showing that, notwithstanding the partial starch
340 hydrolysis, the total NSCs contents were only slightly affected, indicating that beech trees were able
341 to counteract a relatively brief and intense “hot” drought event by the interconversion between
342 starch and soluble sugars without drastically affecting the total C storage reserves in woody tissue.
343 This extreme weather event delayed the starch accumulation in woody tissue during the late
344 summer-autumn period, when storage carbohydrates represent one of the major forest C sinks
345 (Scartazza *et al.*, 2013). However, at the end of the 2017 vegetative season, trees were able to store
346 similar amounts of starch and total NSCs compared to the modelled reference value of the site,
347 confirming that the studied forest showed an efficient internal regulation mechanism able to
348 respond to environmental factors with short- to medium-term homeostatic equilibrium (Scartazza *et*
349 *al.*, 2013; Dietrich *et al.*, 2018). The absence of a strong depletion of NSCs even during two
350 sequential years characterised by extreme weather events that strongly reduced C supply and, at the
351 same time, increased C demand for sustaining stress-recovery (frost) and stress-tolerance (drought)
352 processes, further support the hypothesis that C reserves in plants can be tightly actively managed.
353 In this view, wood NCS synthesis, cleavage, interconversion, mobilisation and allocation need to be
354 actively controlled at the physiological biochemical and molecular level, to optimize growth and
355 survival in the long-term (Sala *et al.* 2012; Collalti *et al.* 2018; Collalti *et al.* 2020).

356

357 **The interplay between carbon reserves and growth**

358 At the Collelongo-Selva Piana beech forest, after leaves development, stem radial growth
359 represents the main C sink during the first part of the vegetative season reaching the maximum rate

360 in July. Along the season in the late summer and early autumn period the photosynthates are mainly
361 allocated to the storage C compounds in woody tissues, as described by the models of carbohydrates
362 intra-annual dynamic and by previous studies (Michelot *et al.*, 2012; Scartazza *et al.*, 2013).

363 The complete canopy destruction in spring 2016 led to a drastic reduction of radial growth
364 without affecting stemwood C reserves dynamic during the first part of the vegetative season,
365 supporting the hypothesis that stem radial growth of diffuse-porous tree species starts soon after leaf
366 expansion and C needs are more likely to be supplied by the new assimilates rather than from the C
367 pool stored within the stem sapwood (Barbaroux & Bréda, 2002; Čufar *et al.*, 2008; Zein *et al.*,
368 2011; Michelot *et al.*, 2012). After the “second” green up in July 2016, the accumulation of C
369 reserves was prioritized over allocating recently fixed C to stem growth.

370 In 2017, at the beginning of vegetative season, the new assimilates produced by the canopy
371 photosynthesis were mainly used for sustaining the stem radial growth, which, differently from
372 2016, reached values of BAI similar to those observed for the reference period (1989-2015). In
373 2017, the extreme summer drought affected NSCs dynamic but had only very limited effects on
374 annual stem radial growth, as already observed for other tree species growing in the Mediterranean
375 area, which adopt a stress avoidance strategy, adjusting the end of xylem growth before potential
376 stressful conditions may occur (e.g. Lempereur *et al.* 2015; Forner, Valladares, Bonal, Granier &
377 Grossiord 2018). Ultimately, our results confirm that for Mediterranean beech, growth is more
378 negatively impacted by spring late frost than summer drought (Gazol *et al.*, 2019).

379 Moreover, our results suggest that in long-term adapted mature beech forests, summer
380 drought has limited effects on stem growth, being it mainly dependent on new photosynthates
381 produced in spring. At the opposite summer drought was reported to have important effects on stem
382 growth of young beech trees (Chuste *et al.*, 2020).

383 In beech trees, the duration of wood formation was found to be positively correlated with
384 increasing latitude, with warmer and drier conditions reducing the length of xylogenesis (Martinez
385 *et al.*, 2016). We speculate that the shorter period of wood formation in the more drought-prone
386 Mediterranean forests, could be also related to a local adaptation of beech to environmental
387 constraints (Jump & Peñuelas, 2007). The reduced sink activity (related to radial growth, wall
388 thickening and lignification) during extreme weather events could be functional to prevent NSCs
389 depletion (Anderegg, 2012; Dietrich *et al.*, 2018). The maintenance of high NSCs concentration and
390 control over NSCs metabolism (e.g. starch hydrolysis) during severe drought events contribute to
391 avoid xylem hydraulic failure and strong damages, as observed conversely in Central European
392 beech (Schuldt *et al.*, 2020). It should be noted that NSCs, including starch, can be rapidly
393 interconverted, ensuring a rapid hexose supply to the hexose phosphate pool. The hexose phosphate

394 pool then supports both metabolic and structural cell requirements for reduced carbon, ranging from
395 glycolysis and respiratory metabolism to cell wall polymer synthesis. On the contrary, assimilates
396 ending up in cell wall components cannot be reclaimed for metabolism, representing, in this respect,
397 almost a dead end, at least in the short period. Hence, under photosynthate famine conditions,
398 prioritization of photosynthate allocation to NSCs, might ensure the maintenance of a sufficient
399 amount of metabolically available reduced carbon. This acclimatory choice seems more
400 conservative than supporting end point-like allocation of photosynthates to cell wall components
401 and ensure a much higher plasticity to support plant response to environmental constraints.
402 Furthermore, allocation of photosynthates to NSCs is less energy costly than building new cell
403 walls polymers (Rodríguez-Calcerrada *et al.*, 2019) again making this choice more conservative in
404 case of reduced source activity. The ability of Mediterranean beech trees to store C reserves also
405 during stressful years could represent an active strategy for optimizing growth and survival and
406 coping with the increasing frequency of extreme weather events.

407 Summarizing, our study elucidated the mechanisms connected to the impact of late frost and
408 summer drought on sink processes (stem and foliage growth, allocation to reserve pool) in a
409 Mediterranean beech forest. Synthesis, cleavage, interconversion, mobilisation and allocation of
410 wood NSCs are all finely regulated processes and play a key role in counteracting the negative
411 effects of both late frost and summer drought, ensuring plant survival and buffering the difference
412 between C supply and demand under extreme weather event conditions. This information suggest
413 that C reserves could be crucial for resilience of beech because of the expected increasing frequency
414 of extreme weather events under the future global changes and may be useful for adaptive future
415 management strategies of beech forests in the Mediterranean area and Europe.

416 **Acknowledgements**

417 The activities of Negar Rezaie at the wood anatomy laboratory of Slovenian Forestry Institute were
418 supported by an Excellence Research Award of the National Research Council of Italy, Department
419 of Biology, Agriculture, and Food Secures (Prot. 71951, 06/11/2017). Collelongo-Selva Piana is
420 one of the sites of the Italian Long-Term Ecological Research network (LTER-Italy), part of the
421 International LTER network (ILTER). Research at the site in the years of this study was funded by
422 the eLTER H2020 project (grant agreement no. 654359).

423

424 **Author contribution**

425 E. D'A., A.S, S.M., N.R., G.M. contributed to the design of the research. Fieldwork was carried out
426 by E. D'A., N.R.. Soluble Sugars Content analysis were performed by S.M., A.B, S.P, and A.S..
427 Data analysis was done by E. D'A, A.S., S.M., data interpretation by all co-authors. The manuscript
428 was written by E. D'A, A.S., S.M., A.C.. All authors read and commented the manuscript.

429 **References**

- 430 **Adams HD, Guardiola-Claramonte M, Barron-Gafford GA, Villegas JC, Breshears DD, Zou**
431 **CB, Troch PA, Huxman TE. 2009.** Temperature sensitivity of drought-induced tree mortality
432 portends increased regional die-off under global-change-type drought. *Proceedings of the National*
433 *Academy of Sciences* **106**: 7063–7066.
- 434 **Aho K, Derryberry D, Peterson T. 2014.** Model selection for ecologists: The worldviews of AIC
435 and BIC. *Ecology* **95**: 631–636.
- 436 **Akaike H. 1974.** A new look at the statistical model identification. *IEEE Transactions on*
437 *Automatic Control* **19**: 716–723.
- 438 **Allevato E, Saulino L, Cesarano G, Chirico GB, D'Urso G, Falanga Bolognesi S, Rita A, Rossi**
439 **S, Saracino A, Bonanomi G. 2019.** Canopy damage by spring frost in European beech along the
440 Apennines: effect of latitude, altitude and aspect. *Remote Sensing of Environment* **225**: 431–440.
- 441 **Anderegg WRL. 2012.** Complex aspen forest carbon and root dynamics during drought A letter.
442 *Climatic Change* **111**: 983–991.
- 443 **Augspurger CK. 2013.** Reconstructing patterns of temperature, phenology, and frost damage over
444 124 years: Spring damage risk is increasing. *Ecology* **94**: 41–50.
- 445 **Barbaroux C, Bréda N. 2002.** Contrasting distribution and seasonal dynamics of carbohydrate
446 reserves in stem wood of adult ring-porous sessile oak and diffuse-porous beech trees. *Tree*
447 *physiology* **22**: 1201–10.
- 448 **Bascietto M, Bajocco S, Mazzenga F, Matteucci G. 2018.** Assessing spring frost effects on
449 beech forests in Central Apennines from remotely-sensed data. *Agricultural and Forest*
450 *Meteorology* **248**: 240–250.
- 451 **Bolte A, Czajkowski T, Coccozza C, Tognetti R, de Miguel M, Pšidová E, Ditmarová Ľ, Dinca**
452 **L, Delzon S, Cochard H, et al. 2016.** Desiccation and Mortality Dynamics in Seedlings of
453 Different European Beech (*Fagus sylvatica* L.) Populations under Extreme Drought Conditions.
454 *Frontiers in plant science* **7**: 751.
- 455 **Bonhomme M, Rageau R, Lacoïnte A, Gendraud M. 2005.** Influences of cold deprivation during
456 dormancy on carbohydrate contents of vegetative and floral primordia and nearby structures of

457 peach buds (*Prunus persica* L. Batch). *Scientia Horticulturae* **105**: 223–240.

458 **Carbone MS, Czimczik CI, Keenan TF, Murakami PF, Pederson N, Schaberg PG, Xu X,**
459 **Richardson AD. 2013.** Age, allocation and availability of nonstructural carbon in mature red maple
460 trees. *New Phytologist* **200**: 1145–1155.

461 **Chaves MM, Maroco J, Pereira JS. 2003.** Understanding plant responses to drought - From genes
462 to the whole plant. *Functional Plant Biology* · **30**: 239–264.

463 **Chuste P-A, Maillard P, Bréda N, Levillain J, Thirion E, Wortemann R, Massonnet C. 2020.**
464 Sacrificing growth and maintaining a dynamic carbohydrate storage are key processes for
465 promoting beech survival under prolonged drought conditions. *Trees* **34**: 381–394.

466 **Collalti A, Marconi S, Ibrom A, Trotta C, Anav A, D'Andrea E, Matteucci G, Montagnani L,**
467 **Gielen B, Mammarella I, et al. 2016.** Validation of 3D-CMCC Forest Ecosystem Model (v . 5 . 1
468) against eddy covariance data for 10 European forest sites. *Geoscientific Model Development* **9**:
469 479–504.

470 **Collalti A, Tjoelker MG, Hoch G, Mäkelä A, Guidolotti G, Heskell M, Petit G, Ryan MG,**
471 **Battipaglia G, Matteucci G, et al. 2020.** Plant respiration: Controlled by photosynthesis or
472 biomass? *Global Change Biology* **26**: 1739–1753.

473 **Collalti A, Trotta C, Keenan TF, Ibrom A, Bond-lamberty B, Grote R, Vicca S, Reyer CPO.**
474 **2018.** Thinning Can Reduce Losses in Carbon Use Efficiency and Carbon Stocks in Managed
475 Forests Under Warmer Climate. *Journal of Advances in Modeling Earth Systems*: 2427–2452.

476 **Čufar K, Prislan P, De Luis M, Gričar J. 2008.** Tree-ring variation, wood formation and
477 phenology of beech (*Fagus sylvatica*) from a representative site in Slovenia, SE Central Europe.
478 *Trees - Structure and Function* **22**: 749–758.

479 **D'Andrea E, Guidolotti G, Scartazza A, Angelis P De, Matteucci G. 2020a.** Small-scale forest
480 structure influences spatial variability of belowground carbon fluxes in a mature mediterranean
481 beech forest. *Forests* **11**: 1–11.

482 **D'Andrea E, Rezaie N, Battistelli A, Gavrichkova O, Kuhlmann I, Matteucci G, Moscatello S,**
483 **Proietti S, Scartazza A, Trumbore S, et al. 2019.** Winter's bite: beech trees survive complete
484 defoliation due to spring late-frost damage by mobilizing old C reserves. *New Phytologist* **224**:
485 625–631.

486 **D'Andrea E, Rezaie N, Prislan P, Gričar J, Collalti A, Muhr J, Matteucci G. 2020b.** Frost and
487 drought: effects of extreme weather events on stem carbon dynamics in a Mediterranean beech
488 forest. *Plant, Cell & Environment*.

489 **Dietrich L, Delzon S, Hoch G, Kahmen A. 2018.** No role for xylem embolism or carbohydrate
490 shortage in temperate trees during the severe 2015 drought. *Journal of Ecology* **107**: 334–349.

491 **Dittmar C, Fricke W, Elling W. 2006.** Impact of late frost events on radial growth of common
492 beech (*Fagus sylvatica* L .) in Southern Germany. *European Journal of Forest Research* **125**: 249–
493 259.

494 **Fatichi S, Leuzinger S, Körner C. 2014.** Moving beyond photosynthesis: from carbon source to
495 sink-driven vegetation modeling. *New Phytologist* **201**: 1086–1095.

496 **Flaounas E, Drobinski P, Vrac M, Bastin S, Lebeau-pin-Brossier C, Stéfanon M, Borga M,
497 Calvet JC. 2013.** Precipitation and temperature space-time variability and extremes in the
498 Mediterranean region: Evaluation of dynamical and statistical downscaling methods. *Climate*
499 *Dynamics* **40**: 2687–2705.

500 **Forner A, Valladares F, Bonal D, Granier A, Grossiord C. 2018.** Extreme droughts affecting
501 Mediterranean tree species' growth and water-use efficiency: the importance of timing. *Tree*
502 *physiology*.

503 **Frank D, Reichstein M, Bahn M, Thonicke K, Frank D, Mahecha MD, Smith P, van der Velde
504 M, Vicca S, Babst F, et al. 2015.** Effects of climate extremes on the terrestrial carbon cycle:
505 Concepts, processes and potential future impacts. *Global Change Biology* **21**: 2861–2880.

506 **Fu J, Fry J. 2010.** Osmotic Potential , Sucrose Level , and Activity of Sucrose Metabolic Enzymes
507 in Tall Fescue in Response to Deficit Irrigation. *Journal of the American Society for Horticultural*
508 *Science* **135**: 506–510.

509 **Gazol A, Camarero JJ, Colangelo M, de Luis M, Martínez del Castillo E, Serra-Maluquer X.
510 2019.** Summer drought and spring frost, but not their interaction, constrain European beech and
511 Silver fir growth in their southern distribution limits. *Agricultural and Forest Meteorology* **278**:
512 107695.

513 **Giorgi F. 2006.** Climate change hot-spots. *Geophysical Research Letters* **33**: 1–4.

514 **Gordo O, Sanz JJ. 2010.** Impact of climate change on plant phenology in Mediterranean
515 ecosystems. *Global Change Biology* **16**: 1082–1106.

516 **Gottardini E, Cristofolini F, Cristofori A, Pollastrini M, Camin F, Ferretti M. 2020.** A multi-
517 proxy approach reveals common and species-specific features associated with tree defoliation in
518 broadleaved species. *Forest Ecology and Management* **467**: 118151.

519 **Guidolotti G, Rey A, D'Andrea E, Matteucci G, De Angelis P. 2013.** Effect of environmental
520 variables and stand structure on ecosystem respiration components in a Mediterranean beech forest.
521 *Tree Physiology* **33**: 960–972.

522 **Hartmann H, Trumbore S. 2016.** Understanding the roles of nonstructural carbohydrates in forest
523 trees - from what we can measure to what we want to know. *The New phytologist* **211**: 386–403.

524 **Hartmann H, Ziegler W, Kolle O, Trumbore S. 2013.** Thirst beats hunger – declining hydration

525 during drought prevents carbon starvation in Norway spruce saplings. *New Phytologist* **200**: 340–
526 349.

527 **Hoch G, Richter A, Körner C. 2003.** Non-structural carbon compounds in temperate forest trees.
528 *Plant, Cell and Environment* **26**: 1067–1081.

529 **Jump A, Peñuelas J. 2007.** Extensive spatial genetic structure revealed by AFLP but not SSR
530 molecular markers in the wind-pollinated tree, *Fagus sylvatica*. *Molecular Ecology*: 925–936.

531 **Ladwig LM, Chandler JL, Guiden PW, Henn JJ. 2019.** Extreme winter warm event causes
532 exceptionally early bud break for many woody species. *Ecosphere* **10**.

533 **Lempereur M, Martin-stpaul NK, Damesin C, Joffre R, Ourcival J, Rocheteau A, Rambal S.**
534 **2015.** Growth duration is a better predictor of stem increment than carbon supply in a
535 Mediterranean oak forest: implications for assessing forest productivity under climate change. :
536 579–590.

537 **Li W, Hartmann H, Adams HD, Zhang H, Jin C, Zhao C, Guan D, Wang A, Yuan F, Wu J.**
538 **2018.** The sweet side of global change—dynamic responses of non-structural carbohydrates to
539 drought, elevated CO₂ and nitrogen fertilization in tree species. *Tree Physiology* **38**: 1706–1723.

540 **Martínez E, Longares LA, Gricar J, Prislan P, Luis M De. 2016.** Living on the Edge: :
541 Contrasted Wood-Formation Dynamics in *Fagus sylvatica* and *Pinus sylvestris* under Mediterranean
542 Conditions. **7**: 1–10.

543 **McDowell NG. 2011.** Mechanisms Linking Drought, Hydraulics, Carbon Metabolism, and
544 Vegetation Mortality. *Plant Physiology* **155**: 1051–1059.

545 **McDowell N, McDowell N, Pockman WT, Allen CD, David D, Cobb N, Kolb T, Plaut J, Sperry**
546 **J, West A, et al. 2008.** Mechanisms of plant survival and mortality during drought: why do some
547 plants survive while others succumb to. *New Phytologist (2008)* **178**: 719–739.

548 **McDowell NG, Sevanto S. 2010.** The mechanisms of carbon starvation: how, when, or does it even
549 occur at all? *New Phytologist* **186**: 264–266.

550 **Merganičová K, Merganič J, Lehtonen A, Vacchiano G, Sever MZO, Augustynczyk ALD,**
551 **Grote R, Kyselová I, Mäkelä A, Yousefpour R, et al. 2019.** Forest carbon allocation modelling
552 under climate change (A Polle, Ed.). *Tree Physiology* **39**: 1937–1960.

553 **Michelot A, Simard S, Rathgeber C, Dufrêne E, Damesin C. 2012.** Comparing the intra-annual
554 wood formation of three European species (*Fagus sylvatica*, *Quercus petraea* and *Pinus sylvestris*)
555 as related to leaf phenology and non-structural carbohydrate dynamics. *Tree Physiology* **32**: 1033–
556 1045.

557 **Morgan JM. 1984.** Osmoregulation and Water Stress in Higher Plants. *Annual Review of Plant*
558 *Physiology* **35**: 299–319.

559 **Moscatello S, Proietti S, Augusti A, Scartazza A, Walker RP, Famiani F, Battistelli A. 2017.**
560 Late summer photosynthesis and storage carbohydrates in walnut (*Juglans regia* L.): Feed-back and
561 feed-forward effects. *Plant Physiology and Biochemistry* **118**: 618–626.

562 **Noce S, Collalti A, Santini M. 2017.** Likelihood of changes in forest species suitability,
563 distribution, and diversity under future climate: The case of Southern Europe. *Ecology and*
564 *Evolution* **7**: 9358–9375.

565 **Nolè A, Rita A, Ferrara AMS, Borghetti M. 2018.** Effects of a large-scale late spring frost on a
566 beech (*Fagus sylvatica* L.) dominated Mediterranean mountain forest derived from the spatio-
567 temporal variations of NDVI. *Annals of Forest Science* **75**: 83.

568 **Nussbaumer A, Meusburger K, Schmitt M, Waldner P, Gehrig R, Haeni M, Rigling A,**
569 **Brunner I, Thimonier A. 2020.** Extreme summer heat and drought lead to early fruit abortion in
570 European beech. *Scientific Reports* **10**: 1–11.

571 **Pastorello G, Trotta C, Canfora E, Chu H, Christianson D, Cheah Y-W, Poindexter C, Chen**
572 **J, Elbashandy A, Humphrey M, et al. 2020.** The FLUXNET2015 dataset and the ONEFlux
573 processing pipeline for eddy covariance data. *Scientific Data* **7**: 225.

574 **Peuke AD, Schraml C, Hartung W, Rennenberg H. 2002.** Identification of drought-sensitive
575 beech ecotypes by physiological parameters. *New Phytologist* **154**: 373–387.

576 **Prislan P, Čufar K, De Luis M, Gričar J. 2018.** Precipitation is not limiting for xylem formation
577 dynamics and vessel development in European beech from two temperate forest sites. *Tree*
578 *Physiology* **38**: 186–197.

579 **Proietti S, Moscatello S, Fagnano M, Fiorentino N, Impagliazzo A, Battistelli A. 2017.**
580 Chemical composition and yield of rhizome biomass of *Arundo donax* L. grown for biorefinery in
581 the Mediterranean environment. *Biomass and Bioenergy* **107**: 191–197.

582 **R Development Core Team. 2018.** R: A Language and Environment for Statistical Computing.

583 **Reyer CPO, Silveyra Gonzalez R, Dolos K, Hartig F, Hauf Y, Noack M, Lasch-Born P, Rötzer**
584 **T, Pretzsch H, Meesenburg H, et al. 2020.** The PROFOUND Database for evaluating vegetation
585 models and simulating climate impacts on European forests. *Earth System Science Data* **12**: 1295–
586 1320.

587 **Rezaie N, D’Andrea E, Bräuning A, Matteucci G, Bombi P, Lauteri M. 2018.** Do atmospheric
588 CO₂ concentration increase, climate and forest management affect iWUE of common beech?
589 Evidences from carbon isotope analyses in tree rings. *Tree Physiology* **1975**: 1110–1126.

590 **Rita A, Camarero JJ, Nolè A, Borghetti M, Brunetti M, Pergola N, Serio C, Vicente-Serrano**
591 **SM, Tramutoli V, Ripullone F. 2019.** The impact of drought spells on forests depends on site
592 conditions: The case of 2017 summer heat wave in southern Europe. *Global Change Biology*: 1–13.

593 **Rodríguez-Calcerrada J, Salomón RL, Gordaliza GG, Miranda JC, Miranda E, de la Riva**
594 **EG, Gil L. 2019.** Respiratory costs of producing and maintaining stem biomass in eight co-
595 occurring tree species. *Tree physiology* **39**: 1838–1854.

596 **Rossi S, Menardi R, Fontanella F, Anfodillo T. 2005.** Campionatore Trephor: un nuovo
597 strumento per l'analisi della xilogenesi in specie legnose. *Dendronatura* **1**: 60–67.

598 **Sala A, Woodruff DR, Meinzer FC. 2012.** Carbon dynamics in trees: Feast or famine? *Tree*
599 *Physiology* **32**: 764–775.

600 **Scartazza A, Moscatello S, Matteucci G, Battistelli A, Brugnoli E. 2013.** Seasonal and inter-
601 annual dynamics of growth, non-structural carbohydrates and C stable isotopes in a Mediterranean
602 beech forest. *Tree physiology* **33**: 730–42.

603 **Scartazza a., Moscatello S, Matteucci G, Battistelli a., Brugnoli E. 2015.** Combining stable
604 isotope and carbohydrate analyses in phloem sap and fine roots to study seasonal changes of source-
605 sink relationships in a Mediterranean beech forest. *Tree Physiology*: 1–11.

606 **Scartazza A, Proietti S, Moscatello S, Augusti A, Monteverdi MC, Brugnoli E, Battistelli A.**
607 **2001.** Effect of water shortage on photosynthesis, growth and storage carbohydrate accumulation in
608 walnut (*Juglans regia* L.). *Acta Horticulturae*: 227–232.

609 **Schuldt B, Buras A, Arend M, Vitasse Y, Beierkuhnlein C, Damm A, Gharun M, Grams TEE,**
610 **Hauck M, Hajek P, et al. 2020.** A first assessment of the impact of the extreme 2018 summer
611 drought on Central European forests. *Basic and Applied Ecology*.

612 **Spinoni J, Naumann G, Vogt J, Barbosa P. 2015.** European drought climatologies and trends
613 based on a multi-indicator approach. *Global and Planetary Change* **127**: 50–57.

614 **Stocker TF, Qin D, Plattner GK, Tignor MMB, Allen SK, Boschung J, Nauels A, Xia Y, Bex**
615 **V, Midgley PM. 2014.** *Climate Change 2013 - The Physical Science Basis* (Intergovernmental
616 Panel on Climate Change, Ed.). Cambridge: Cambridge University Press.

617 **Tixier A, Guzmán-Delgado P, Sperling O, Amico Roxas A, Laca E, Zwieniecki MA. 2020.**
618 Comparison of phenological traits, growth patterns, and seasonal dynamics of non-structural
619 carbohydrate in Mediterranean tree crop species. *Scientific Reports* **10**: 347.

620 **Tixier A, Sperling O. 2015.** Temperature-assisted redistribution of carbohydrates. *American*
621 *Journal of Botan* **102**: 1216–1218.

622 **Vitasse Y, Schneider L, Rixen C, Christen D, Rebetez M. 2018.** Increase in the risk of exposure
623 of forest and fruit trees to spring frosts at higher elevations in Switzerland over the last four
624 decades. *Agricultural and Forest Meteorology* **248**: 60–69.

625 **Witt W, Sauter JJ. 1994.** Starch metabolism in poplar wood ray cells during spring mobilization
626 and summer deposition. *Physiologia Plantarum* **92**: 9–16.

627 **Yang Z. 2013.** Changes in Carbohydrate Metabolism in Two Kentucky Bluegrass Cultivars
628 Changes in Carbohydrate Metabolism in Two Kentucky Bluegrass Cultivars during Drought Stress
629 and Recovery. *American Society for Horticultural Science* **138**: 24–30.

630 **Zein R El, Maillard P, Bréda N, Marchand J, Montpied P, Gérant D. 2011.** Seasonal changes
631 of C and N non-structural compounds in the stem sapwood of adult sessile oak and beech trees.
632 *Tree physiology* **31**: 843–854.

633 **Zhang X, Friedl M a., Schaaf CB, Strahler AH, Hodges JCF, Gao F, Reed BC, Huete A. 2003.**
634 Monitoring vegetation phenology using MODIS. *Remote Sensing of Environment* **84**: 471–475.

635 **Zohner CM, Mo L, Renner SS, Svenning J-C, Vitasse Y, Benito BM, Ordonez A, Baumgarten**
636 **F, Bastin J-F, Sebald V, et al. 2020.** Late-spring frost risk between 1959 and 2017 decreased in
637 North America but increased in Europe and Asia. *Proceedings of the National Academy of Sciences*
638 **117**: 12192–12200.

639
640

641
642
643
644
645
646

647
648
649
650
651
652
653
654
655
656
657
658
659
660
661
662
663
664
665
666
667
668
669
670

Table 1: Parameters of the polynomial model describing the intra-annual variation of non-structural carbohydrates (total sugars, starch and soluble sugars content) in beech wood, n is the number of samplings used for the analysis and RMSE ($\text{mg g}_{\text{DW}}^{-1}$) is the root mean square error.

Components	yo	a	b	c	d	e	n	R ²	RMSE	p-value
Total sugars	28.29	11.21	-5.47	-3.68	-10.23	4.95	28	0.64	2.36	<0.001
Starch	19.55	4.98	-26.09	2.43	-14.76	-	39	0.78	2.57	<0.001
Soluble sugars	9.41	8.13	20.28	-3.31	1.72	-3.97	28	0.93	1.00	<0.001

671 **Figure legends**

672 **Figure 1:** Deviations of monthly mean temperature and precipitation for 2016 (blue bars, panel A)
673 and 2017 (red bars, panel B) calculated as the difference from the 2000-2015 average value at the
674 site. Temperature of April 25th, 2016 measured at canopy level (24 m) is reported in inset graph of
675 panel *a*, while the annual precipitation of the year 2016 (blue dots), 2017 (red dots) and the long-
676 term average (black dots) is reported in the inset graph of panel *b*.

677

678 **Figure 2:** Seasonal dynamics of Leaf area index (LAI, $\text{m}^2 \text{m}^{-2}$, panel *a*) and daily stem radial
679 increment (panel *b*) for the years 2016, 2017 and the 2000-2015 reference period. LAI was derived
680 from Moderate Resolution Imaging Spectroradiometer (MODIS, see Materials and Methods), for
681 2016 (blue line), 2017 (red line) and for the 2000-2015 reference period (black line). Solid lines are
682 the modelled LAI pattern, using two logistic functions for the increasing and decreasing phases.
683 Dots are the raw MODIS-LAI values. In panel *b* the daily radial increment for 2016 (blue dots) and
684 2017 (red dots) are shown, while the inset graph reports the long-term series data of Basal Area
685 chronology (BAI, $\text{cm}^2 \text{year}^{-1}$), where the last two dots represent the BAI value obtained in 2016
686 (blue dot) and 2017 (red dot), respectively.

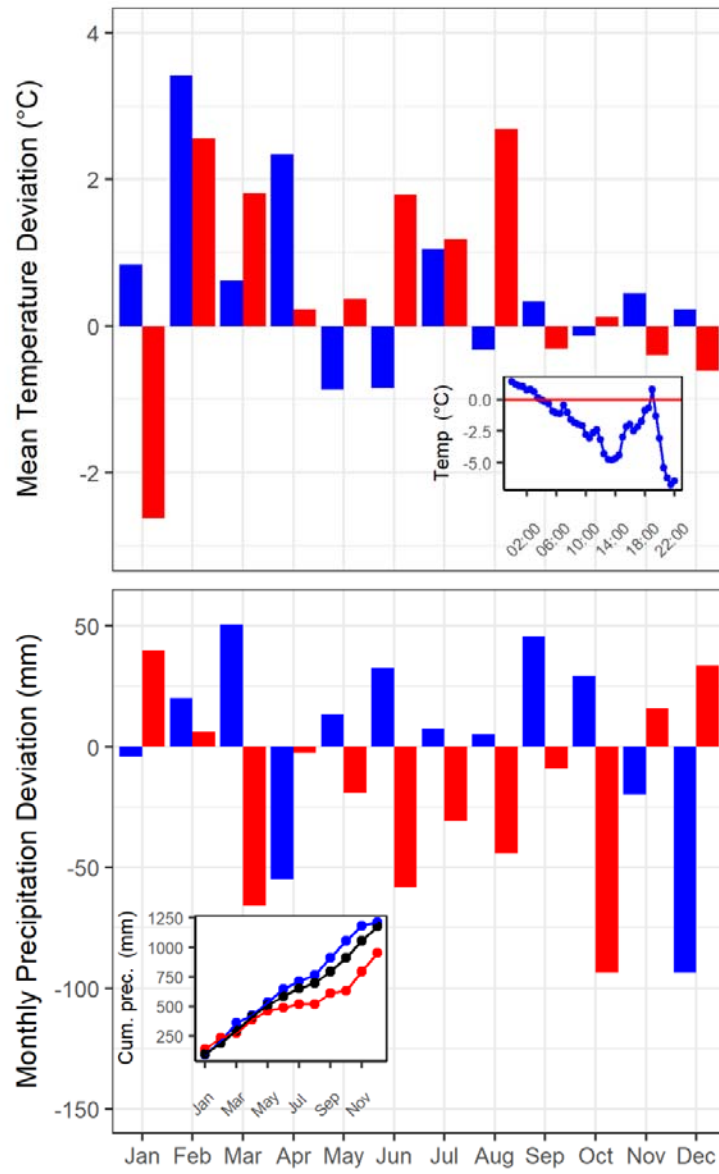
687

688 **Figure 3:** Phenological data for the experimental beech forest site (top panel) and seasonal dynamic
689 of NSCs content as total NSCs (panel *a*), starch (panel *b*) and soluble sugars (panel *c*). In the top
690 panel, the different colours represent dormancy (dark orange), the period between the green up and
691 the maximum Leaf area index (LAI, $\text{m}^2 \text{m}^{-2}$) value (light green), the maximum LAI (dark green),
692 the senescence phase (light orange) and, finally, the leafless period after the late frost in 2016
693 (grey). In the panels *a*, *b*, and *c*, blue and red dots represent carbohydrate concentrations of 2016
694 and 2017, respectively, while the black lines and grey area show modelled intra annual dynamic of
695 carbohydrates and interval of confidence, respectively. Each point is the mean of five beech trees
696 and bars are the standard errors (see Material and Methods). Modelled values are derived from 39
697 and 28 measurements of starch and soluble sugar content, respectively.

698

699 **Figure 1**

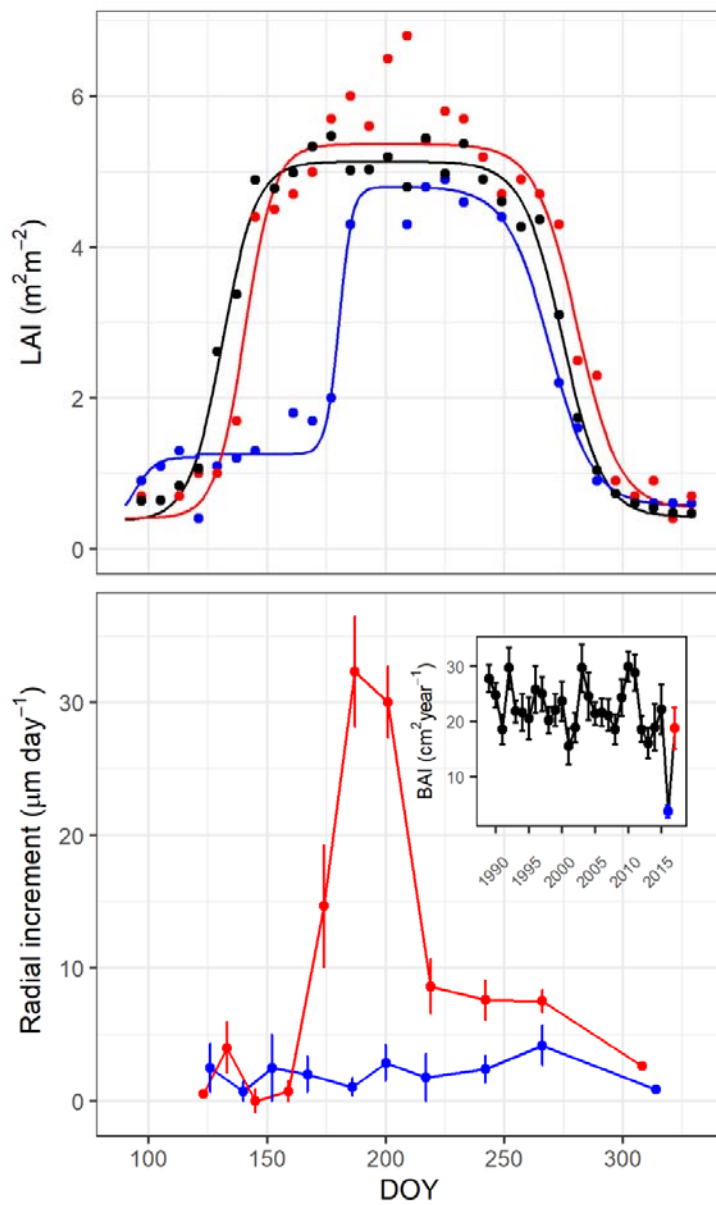
700



701

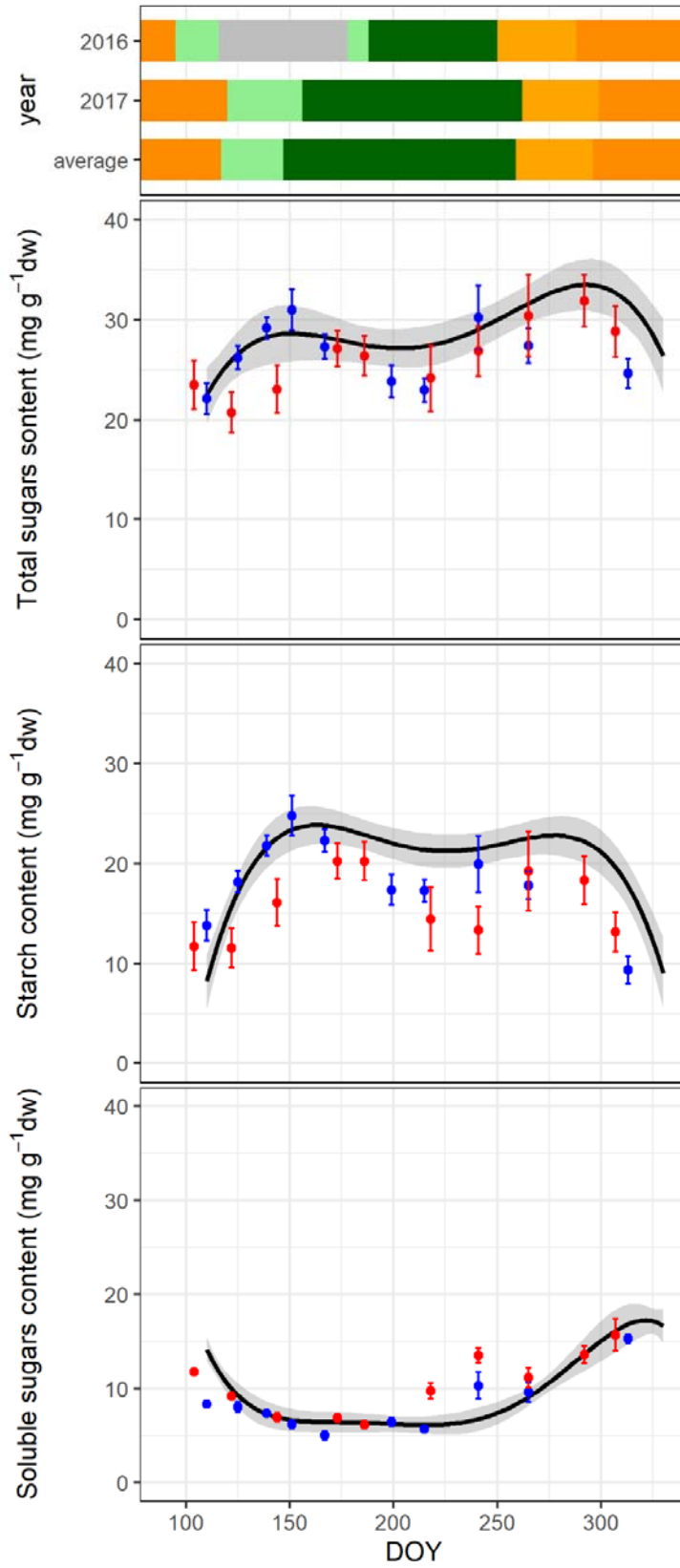
702

703 **Figure 2**



704

705



708 **Supporting Information**

709

710 **Table S1:** Dataset of soluble sugar (glucose, fructose and sucrose), starch and total non-structural
711 carbohydrates.